IEEE Access
Multidisciplinary | Rapid Review | Open Access Journal

Received March 18, 2021, accepted April 12, 2021, date of publication May 4, 2021, date of current version May 13, 2021.

Digital Object Identifier 10.1109/ACCESS.2021.3077554

Invariant Incoherent MIMO Reception Over Doubly Selective Channels

G. RAMIREZ-ARREDONDO[1], F. PEÑA-CAMPOS[2], RAMON PARRA-MICHEL[1], AND VALERI KONTOROVICH[3], (Life Fellow, IEEE)

[1]Department of Electrical Engineering, Centro de Investigación y de Estudios Avanzados (CINVESTAV), Zapopan 45017, México
[2]EIC Mecatrónica, Tecnológico de Monterrey, Zapopan 45201, México
[3]Department of Communications, Centro de Investigación y de Estudios Avanzados (CINVESTAV), Mexico City 07360, México

Corresponding author: G. Ramirez-Arredondo (gramireza@gdl.cinvestav.mx)

This work was supported by the Consejo Nacional de Ciencia y Tecnología (CONACyT) under Grant 300971.

ABSTRACT Nowadays, there is a need for wireless communications to operate over a variety of scenarios, including high mobility multiple-input multiple-output (MIMO) applications, that bring along a challenging problem. In channels where Doppler spread and delay spread are high, complexity of coherent detectors and pilot overhead are both raised. This work proposes a non-coherent reception technique, easily scalable to any number of antennas for the MIMO case, using simple coding and decoding structures which take advantage of channel diversity addition in three domains: time, frequency and space, by using virtual trajectories along with space time block-coding. Coarse analytics on the system performance in terms of the bit error rate are computed using Chernoff Boundaries as a function of the channel diversity and the order of the differential modulation, validating the efficiency of the proposed receiver.

INDEX TERMS Differential modulation, doubly selective channels, invariance, MIMO, non-coherent receivers, space-time coding.

I. INTRODUCTION

Requirements for New Radio (5G and beyond) mobile communication systems include establishing communication in Doubly Selective Channels (DSC). This posses some key challenges for system design that need to be faced, as seen in [1].

1) Fast time-varying fading: The fast time variations of the channels must be taken into consideration, because a large Doppler spread can result from this phenomenon. Wireless communications are designed to operate at certain frequencies and for high-mobility scenarios, the Doppler shift can even reach the thousands of Hz order.

2) Channel estimation errors: In high mobility environments, the fast changing of the channel response, makes the channel estimation process a quite challenging task. Obtaining the Channel State Information (CSI) is no longer a viable option, particularly, if the multiple-input, multiple-output (MIMO) case is considered, it could result in an even worse scenario, where the useful payload will be diminished because of the great amount of a priori information needed to perform the channel estimation.

3) Doppler diversity: Fast time-varying channels are rich in Doppler diversity, which is difficult to exploit by a coherent receiver without an accurate estimation algorithm.

This work focuses mainly on the mitigation of the aforementioned problems. The solution incorporates differential phase modulation over a system that exploits the doubly-selective channel orthogonalization using the so-called virtual trajectories [2]–[4]. Moreover, the approach in this work relies on a low-complexity incoherent detector that provides simple scalability with the number of antennas in the MIMO array.

Most of the work related to overcoming highly time-varying MIMO channels focuses on the coherent reception [5]–[8]. However, in the upcoming generations of communications systems, the common assumption of having accurate CSI will not hold up [1].

On the other hand, non-coherent reception is a viable solution given that no CSI is necessary, which can save processing time at the receiver and alleviate the need for pilot symbols.

The associate editor coordinating the review of this manuscript and approving it for publication was Jiayi Zhang.

By choosing a proper signal shape (modulation and coding) it is possible to neglect the influence of the channel "imperfections" at the desired signal reception. One of the opportunistic trends is the application of Differential Modulation methods, particularly Differential Phase Shift Keying (DPSK) modulation [9]–[11].

DPSK offers attractive characteristics against channel distortions, which depend on the differential order of modulation; particularly, invariance (strictly speaking, conditional invariance) to certain impairments of the channel can be achieved [9]. It is well known that DPSK of the first order presents invariance to the initial phase introduced by the channel, and the second order offers invariance to the Doppler shift effect in Single-Input Single-Output (SISO) communication channels [9], [12]. In addition to phase invariance, DPSK offers simple detection by means of the autocovariance algorithm.

There are several works that consider DPSK applications. In [13], a differential modulation for the SISO case over Rayleigh channels is proposed, taking advantage of non-coherent receivers. In [14] a diversity-encoded Differential Amplitude Phase Shift Keying (DAPSK) for Orthogonal Frequency Division Multiplexing (OFDM) is used; other applications of differential modulation include [15]–[18] and [19]. It is worth mentioning that none of these references take into consideration DSC. In [3] a non-coherent receiver is proposed, considering only the SISO case.

For the MIMO case, a differential space time modulation for a 2×2 antenna array is proposed in [11]. Later on, [10] presents a double differential space-time block coding for time-selective fading channels that also use unitary group coding matrices, which can be scaled to a desired $N \times N$ MIMO antenna arrangement; however, it has the limitation of using a sub-optimal Maximum Likelihood (ML) detector, which highly increases the complexity at the receiver. In [20], a differential encoding is proposed for Orthogonal Space Time Block Coding (OSTBC) using the MIMO case and different decoding methods. Recently, results from applying first order DPSK incoherent reception in high-mobility double-selective channels are presented in [4], with the particular application of a differential block code on a 2×2 MIMO system along with other coherent receivers.

After an analysis of the state of the art, a great opportunity is presented, given that there are few approaches available focusing their efforts on DSC, which are practically unavoidable in modern communication scenarios.

The aim of this work is to provide a generalized solution with a simple non-coherent receiver, which can be implemented in any $N \times N$ MIMO system. Invariance to the influence of the doubly selective channel is achieved by an autocovariance detector along with the implementation of a virtual trajectories receiver with space-frequency-Doppler energy addition.

The results in terms of noise immunity evaluation of the Bit Error Rate (BER) probability, using Chernoff Boundaries, are presented. The analysis shows its capability for predicting the performance for the SISO and MIMO cases with acceptable accuracy using DPSK and the virtual trajectories addition method.

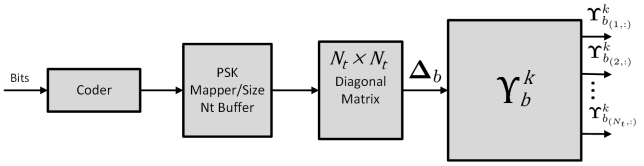

FIGURE 1. Transmitter.

Additional time and frequency diversity is exploited by the application of well-known channel coding methods in [12], [21].

The structure of this paper is as follows: Section II presents the generalization for the transmitter, receiver and the system model for the MIMO case; Section III develops the upper Chernoff boundaries for the noise immunity in the SISO and MIMO cases, generalized for any DPSK order. In Section IV, the simulation and results are presented. Final conclusions of the proposed approach are presented in Section V.

The notation that is going to be used through this work can be seen hereafter: Bold lower (upper) case letters are used to denote vector (matrices); $(\cdot)^T$ and $(\cdot)^H$ denote transpose and Hermitian, respectively; $\langle\cdot\rangle_N$ denotes modulus N number evaluation. $D(x)$ denotes a diagonal matrix with entry x. $A^\dagger$ is the Moore-Penrose pseudoinverse of matrix A, while $[\mathbf{H}]_{k,l}$ is the $l-th$ element in the $k-th$ row of matrix $\mathbf{H}$.

II. SYSTEM MODEL. DPSK FOR THE MIMO CASE

Let the diagram in Fig. 1 present the transmitter architecture. For the first stage (coder), the information arrives as bits. The coding method is left to the user, depending on the system requirements.

In the second block, the mapping of the symbol is dependent on the constellation cardinality as:

$$\log_2(M)_{bits} \leftrightarrow s_i \quad \forall i \in [0, M-1]. \tag{1}$$

In order to form the STBC of size $N_t \times N_r$, N_t of the constellation symbols are taken into consideration, where N_t and N_r are the number of transmitting and receiving antennas, respectively, and for this case $N_t = N_r$. These symbols will form the matrix

$$\mathbf{\Delta}_b = \begin{bmatrix} s_{N_t(b+1)-1} & \cdots & 0 \\ \vdots & \ddots & \vdots \\ 0 & \cdots & s_{N_t(b+1)-1} \end{bmatrix}, \tag{2}$$

where b represents the variable to index the matrix containing $N_t \times N_t$ symbols. $[s_{N_t(b+1)-1} \cdots s_{N_t(b+1)-1}]$ are the symbols associated with the matrix $\mathbf{\Delta}$ in the time instant indexed as b.

The matrix in equation (2) is used to perform a differential modulation; it can be of any order, but the first order is presented as:

$$\mathbf{\Upsilon}_b^1 = \mathbf{\Upsilon}_{b-1}^1 \mathbf{\Delta}_b, \tag{3}$$

where $\mathbf{\Upsilon}_b^1$ is the differentially modulated matrix, 1 is the order of the DPSK, and as initial condition $\mathbf{\Upsilon}_0^1 = \mathbf{I}$ or it could be an orthonormal matrix (the Fourier matrix, e.g.) or any other that fulfills the condition $\mathbf{PP}^H = \mathbf{I}$. Matrix $\mathbf{\Upsilon}_b^1$ is defined as: $\mathbf{\Upsilon}_b^1 = [\boldsymbol{v}_{b,1}^T, \boldsymbol{v}_{b,2}^T \cdots \boldsymbol{v}_{b,N_t}^T]$, where $\boldsymbol{v}_{b,N_t}^T$ are the columns of the differentially modulated matrix. High-order differential modulation is performed with the concatenation of the matrix structure in (2) and, if a whole matrix is to be used to gather diversity, the last concatenated differential modulator must contain the orthonormal matrix as the initial condition.

Each of the rows in equation (3) are sent to a different antenna; this will allow an interchangeable modulation scheme to be used as desired (Single Carrier (SC), OFDM, Virtual Trajectories (VT), etc.).

After going through the channel, the complex base band model of the signal arriving to the ρ-th antenna of the receiver for a single block, indexed by b, is described as:

$$y_\rho[n] = \sum_{\iota=0}^{N_t-1} \sum_{l=0}^{L_{tap}-1} h[\iota, \rho; n, l] \upsilon_\iota \left[\langle \text{n-l} \rangle_N\right] + \xi_\rho[n], \quad (4)$$

where $n = 0, \cdots, N-1$, $\rho = 0, \cdots, N_r - 1$, $\upsilon_\iota[n]$ is the signal from the ι-th transmitter antenna, L_{tap} is the number of channel taps, and $\xi_\rho[n]$ is the additive Gaussian noise with a circular complex delta correlation function on the ρ-th receiving antenna. Then, a compact matrix-vector form of (4) can be presented as:

$$\mathbf{y}_\rho = \sum_{\iota=0}^{N_t-1} \mathbf{H}(\iota, \rho)\boldsymbol{\upsilon}_\iota + \boldsymbol{\xi}_\rho \quad (5)$$

where

$$\mathbf{y}_\rho = \begin{bmatrix} y_\rho[0] & y_\rho[1] & \cdots & y_\rho[N-1] \end{bmatrix}^T \quad (6)$$

$$\boldsymbol{\xi}_\rho = \begin{bmatrix} \xi_\rho[0] & \xi_\rho[1] & \cdots & \xi_\rho[N-1] \end{bmatrix}^T \quad (7)$$

$$\boldsymbol{\upsilon}_\iota = [\upsilon_\iota[0] \quad \upsilon_\iota[1] \quad \cdots \quad \upsilon_\iota[N-1]]^T \quad (8)$$

$$[\mathbf{H}(\iota, \rho)]_{n,n'} = h[\iota, \rho; n, \langle n - n' \rangle_N], \quad (9)$$

where $n' = 0, \cdots, N-1$, $\langle \cdot \rangle_N$ denotes modulus N number evaluation, and the channel impulse response $h[\iota, \rho; n, l]$ for the ι-th transmitter antenna to the ρ-th receiver antenna is assumed to be a random process with zero mean and unknown second order statistics.

In narrowband channels, $\mathbf{H}(\iota, \rho)$ is a diagonal matrix; in the general case, the time and frequency selectivity make $\mathbf{H}(\iota, \rho)$ a banded non-circulant matrix that introduces interference in both domains.

In [4], the Basis Expansion Modeling (BEM) is developed in detail.

The compact I/O model can be defined as:

$$\boldsymbol{y}_\rho = \sum_{\iota,\rho,r,q \in S} \gamma_{\iota,\rho,r,q} \mathbf{G}(r, q)\mathbf{T}\boldsymbol{s}_\iota + \boldsymbol{\xi}_\rho, \quad (10)$$

where, $\gamma_{a,b,r,q}$ are the coefficients for the basis expansion, S is the multi-index space for variables a, b, r and q. $\mathbf{T}_{n,i} = [t_i[n]]$ is the transmitted scheme used, and $\mathbf{s} = [s_1, s_2, \cdots, s_N]$ is a vector containing the transmitted symbols. Now, the channel response of $Tx - Rx$ coupling is defined as:

$$[\mathbf{G}(r, q)]_{n,n'} = \phi_q^I[n]\phi_r^{II}\left[\langle n - n' \rangle_N\right], \quad (11)$$

where $\phi_q^I[n]$ and $\phi_r^{II}[n]$ are the basis functions for the time-delay and time respectively. The prolate basis fits well in both the Doppler and delay domains [4], with the number of coefficients used for the delay and Doppler domains set by M_τ and M_D respectively.

The transmitter has the basic structure of MIMO-OFDM, with orthogonal complex exponential functions:

$$t_i[n] = \exp\left(j2\pi k_i n/N\right), \quad (12)$$

and the carrier allocation rule $k_i = iM_D - N/2$. Then, the observation equation becomes

$$\upsilon_\rho[n] = \sum_{\iota=0}^{N_t-1} \sum_{q=0}^{M_D-1} \sum_{i=0}^{N-1} \vartheta_{\iota,\rho,q}^i \lambda_q^i[n] + \xi_\rho[n], \quad (13)$$

where

$$\vartheta_{\iota,\rho,q}^i = s_{\iota,i} \sum_{r=0}^{M_\tau-1} \gamma_{\iota,\rho,r,q}\varphi_r^i, \quad (14)$$

$$\varphi_r^i = \sum_{l=0}^{L_{tap}-1} \phi_r^{II}[l] \exp\left(-j2\pi k_i n/N\right), \quad (15)$$

$$\lambda_q^i[n] = \phi_q^I[n]t_i[n]. \quad (16)$$

Now, equation (13), can be written in matrix-vector notation

$$\boldsymbol{\upsilon}_\rho = \sum_{\iota=0}^{N_t-1} \mathbf{\Lambda}\mathbf{\Omega}(\iota, \rho)\boldsymbol{s}_\iota + \boldsymbol{\xi}_\rho \quad (17)$$

where the virtual transfer functions are encapsulated as:

$$\mathbf{\Omega}(\iota, \rho) = \left[D(\mathbf{\Gamma})\boldsymbol{\gamma}_{\iota,\rho,0}, \cdots, D(\mathbf{\Gamma})\boldsymbol{\gamma}_{\iota,\rho,M_D-1}\right]^T. \quad (18)$$

where $[\Gamma]_{i,r} = \phi_r^i$, and $\boldsymbol{\gamma}_{\iota,\rho,q} = [\gamma_{\iota,\rho,q,0}, \cdots, \gamma_{\iota,\rho,q,M_\tau-1}]^T$. Double selectivity of each SISO channel is captured in the deterministic matrix:

$$\mathbf{\Lambda} = \left[\mathbf{\Lambda}_0, \mathbf{\Lambda}_1, \cdots, \mathbf{\Lambda}_{M_D-1}\right], \quad (19)$$

where $[\mathbf{\Lambda}_q]_{n,i} = \lambda_q^i[n]$.

Then, applying a pseudo inverse of the deterministic matrix $\mathbf{\Lambda}$:

$$\mathbf{\Lambda}^\dagger = \left(\mathbf{\Lambda}^H\mathbf{\Lambda}\right)^{-1}\mathbf{\Lambda}, \quad (20)$$

provides the observation model:

$$\widehat{\boldsymbol{\vartheta}}_\rho = \mathbf{\Lambda}^\dagger\mathbf{y}_\rho \approx \sum_{\iota}^{N_t-1} \mathbf{\Omega}(\iota, \rho)\mathbf{s}_\iota + \widehat{\boldsymbol{\xi}}_\rho. \quad (21)$$

Now, the received subcarriers in the VTs of the ρ-th receiver-mode and q-th Doppler-mode can be rewritten as:

$$\widehat{\boldsymbol{\vartheta}}_{\rho,q} = \sum_{\iota=0}^{N_t-1} D(\Gamma)\boldsymbol{\gamma}_{\iota,\rho,q}\mathbf{s}_\iota + \widehat{\boldsymbol{\xi}}_{\rho,q}. \quad (22)$$

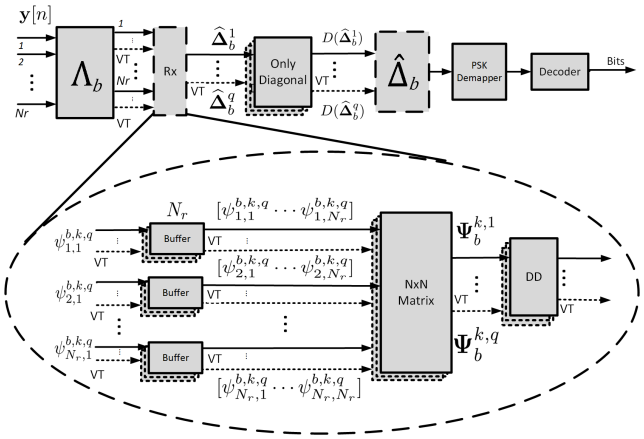

FIGURE 2. Receiver.

This observation model with diagonalized gains on the transmitted symbols is equivalent to the MIMO-OFDM frequency domain I/O relation in time-invariant channels.

Taking into consideration three possible modulation schemes, SC, OFDM and VT in the diagram in Fig. 2 if $\mathbf{\Lambda} = \mathbf{I}$, then SC is used; if $\mathbf{\Lambda} = \mathbf{F}$, OFDM is used ($\mathbf{F}$ is the Fourier Matrix); if $\mathbf{\Lambda} = \mathbf{\Lambda}^{\dagger}$ in equation (20), then VT is used. This provides high flexibility due to the lack of change in the structure at the receiver for different modulation schemes.

If OFDM or SC is selected, the diagram in Fig. 2 can be followed directly, but when VT is used, it must be taken into account that every virtual trajectory must perform the operations inside the dotted circle, which consists of a buffer that allows an $N_r \times N_r$ matrix to be formed as

$$\mathbf{\Psi}_b^{k,q} = \begin{bmatrix} \psi_{1,1}^{b,k,q} & \cdots & \psi_{1,N_r}^{b,k,q} \\ \vdots & \ddots & \vdots \\ \psi_{\rho,1}^{b,k,q} & \cdots & \psi_{\rho,N_r}^{b,k,q} \end{bmatrix}, \tag{23}$$

where

$$\psi_{\rho}^{b,k,q}[n] = \widehat{\vartheta}_{\rho,q}^{b}[n], \tag{24}$$

$\widehat{\vartheta}_{\rho,q}^{b}[n]$ are the symbols associated with the indexed time b and k is the DPSK order.

Then, an extension of the autocovariance demodulator is calculated in the block labeled *DD*. The matrix form of the demodulator allows all the information to be gathered among the antennas, if the orthonormal matrix was used as initial condition at the transmitter. By doing this, the diversity in time, frequency and space can be exploited. The reception process is described as:

$$\widehat{\mathbf{\Delta}}_b^q = (\mathbf{\Psi}_b^{1,q})(\mathbf{\Psi}_{b-1}^{1,q^H}), \tag{25}$$

where $\widehat{\mathbf{\Delta}}_b^q$ is the estimated transmitted matrix over a b time interval and q is the q-th virtual trajectory. This provides a direct extension of an autocovariance demodulator but for the MIMO case. If only a diagonal matrix were sent as useful information, as in equation (2), then the equation would be modified; in this way, the other antennas do not provide any additional information to the receiver. Then, it can be presented as:

$$\widehat{\mathbf{\Delta}}_b^q = (\mathbf{I} \circ \mathbf{\Psi}_b^{1,q})(\mathbf{I} \circ \mathbf{\Psi}_{b-1}^{1,q^H}), \tag{26}$$

where $\circ$ represents the Hadamard product.

Up to this part, if VT was used, every single one of the virtual trajectories must go through each one of these steps inside the small dotted box in the diagram. So, after all of them have completed the process, a combining is performed, where each symbol of the diagonal is added to its counterpart in the other virtual trajectories, as:

$$\widehat{\mathbf{\Delta}}_b = D(\widehat{\mathbf{\Delta}}_b^1) + D(\widehat{\mathbf{\Delta}}_b^2) \cdots D(\widehat{\mathbf{\Delta}}_b^q). \tag{27}$$

This will provide the gathering of diversity and all the benefits that VT has to offer. If no VT were used, then this addition would be omitted. Note that when applying incoherent combining for all possible diversity branches, one quickly encounters the effect of *channel hardening* [22], which drastically simplifies the problem of channel encoding (decoding); actually, it shifts it into a routine encoding for constant channels, practically without memory, in order to diminish BER and energy losses [12]. The choice of a concrete code for such a scenario is well established [12]; see the simulation results as well. That is why hereafter this problem will not be considered in detail.

The last part of the diagram consists of the Phase Shift Keying (PSK) demapper and the channel decoder block, that provides the final estimate of the received bits.

TABLE 1. Complexity comparison.

Method	Complexity
AC (Proposed)	$\mathcal{O}(k_c N_r^2 + M + N_{cod}^2)$
AC-VT (Proposed)	$\mathcal{O}(k_c N_r^2 + M + N_{cod}^2)$
SO-ML [10]	$\mathcal{O}(((5N_{block}^2 + N_{block})M)N_r)$

A. COMPUTATIONAL COMPLEXITY

Since working with an optimum or sub-optimum receiver is questionable for real time implementation [10], the autocovariance receiver comes as a good proposal in order to improve computational complexity.

There is a change in the complexity of the processing algorithm, which can be seen in Table 1.

In the previous table, AC represents the Auto Covariance receiver proposed in this work, AC-VT is the Auto Covariance with a Virtual Trajectories receiver, the SO-ML is the SubOptimum - Maximum Likelihood algorithm used in [10], N_{cod} is the number of bits that the decoder needs, M is the size of the constellation, N_{block} is the size of the block needed to perform the Sub-optimum ML decoder, N_r is the number of receiving antennas and k_c represents a complexity constant that is defined as $k_c = N_{cod}/(N_r \times \log_2(M))$.

The sub-optimum system in [10] states that N must be at least of size N_r; this will result, in the best-case scenario, in a

TABLE 2. Number of operations, with "k" standing for thousands (kilos).

	$Nr = 2$	4	8	16
AC (P) $M = 4$	996	1027	1089	1213
SO-ML $M = 4$ [10]	176	1344	10k	82k
AC (P) $M = 8$	990	1010	1052	1134
SO-ML $M = 8$ [10]	352	2688	20k	165k

complexity of $\mathcal{O}((5N_r^3 + N_r^2)M)$. In Table 2, the number of operations required for different sizes of antennas and two different sizes of constellations $M = 4, 8$ are presented. With the proposed method, a clear advantage can be seen over the sub-optimum proposal, especially with a high number of receiving antennas, where "(P)" stands for "Proposed".

B. GENERALIZATION

Due to the invariance properties that it provides, it is worth generalizing differential modulation and demodulation for the MIMO case for any order, not only DPSK-1 and DPSK-2 as found in the literature. The following lemma will serve for that purpose:

Lemma 1: Let $\mathbf{\Delta}_b$ be a space-time modulated matrix of size $n \times n$, which represents the possible transmitted data in a certain time interval b, and let $\mathbf{\Upsilon}_b^k$ be a differential modulated matrix of order k, defined as

$$\mathbf{\Upsilon}_b^k = f_w(\mathbf{\Upsilon}^{k-1}) = f_{w-1}(\mathbf{\Upsilon}^{k-2}) = \cdots = f_2(\mathbf{\Upsilon}^1) = f_1(\mathbf{\Delta}). \tag{28}$$

Then for demodulation, estimated data $\widehat{\mathbf{\Delta}_b}$ can be calculated as

$$\widehat{\mathbf{\Delta}_b} = f_{z+1}(\mathbf{Y}) = f_z(\mathbf{\Psi}^k) = \cdots = f_2(\mathbf{\Psi}^2) = f_1(\mathbf{\Psi}^1), \tag{29}$$

where Ψ^k is the received space modulated matrix regardless of the order of k.

Proof of the lemma can be found in Appendix A.

C. SIGNAL CONSTRUCTION AND RECEPTION

In the differential modulation model proposed in this work, construction of the functions $f_w(\mathbf{\Upsilon}^k)$ and $f_z(\mathbf{\Psi}^k)$ is the main issue.

The structure of these matrices is based on the binomial coefficients. Function $f_w(\mathbf{\Upsilon}^k)$ will take the case when $(a+c)^r$ and function $f_z(\mathbf{\Psi}^k)$ when $(a-c)^r$.

For the modulation case, the binomial coefficients are presented in equation (30), as shown at the bottom of the page and for the demodulation, they are stated by equation (31), as shown at the bottom of the page, where κ^{+r} and κ^{-r} are the vectors containing the coefficients for constructing the matrices for modulation and demodulation, respectively. The coefficients will represent the number of times a matrix is multiplied by itself and the position of the coefficient in the vector κ^{+r} and κ^{-r} will indicate the time instant.

Any function $f_w(\mathbf{\Upsilon}_b^k)$ can be constructed with matrices of the lowest order $k = 1$. To do this, κ^{+r} and κ^{-r} must be calculated when $r = k$, so that the coefficients represent the necessary multiplications of matrices $\mathbf{\Upsilon}^1$, which is presented in equation (32), as shown at the bottom of the page.

The substitution can be done directly and construct any order of differential modulation with a function of the matrix of symbols sent in STBC. If there is a need to calculate the representation of $f_w(\mathbf{\Upsilon}^k)$ in terms of some matrix $\mathbf{\Upsilon}^{k-p}$, then $r = p + 1$ is used to calculate the coefficients in κ^{+r}.

For the demodulation, the same process occurs; once the coefficients κ^{-r} are calculated, a matrix of estimated data $\widehat{\mathbf{\Delta}}_b$ for a k order of differential modulation can be achieved with a function

$$f_z(\mathbf{\Psi}^k) = f_{z-1}(\mathbf{Y}), \tag{33}$$

where $\mathbf{Y}$ is the received data matrix in each antenna during a certain period of time. Then, with some mathematical work it can be seen that

$$\widehat{\mathbf{\Delta}}_b = f_z(\mathbf{\Psi}^k). \tag{34}$$

When a representation is desired with $\mathbf{\Psi}^1$, the condition $r = k$ must hold for the calculation of coefficients κ^{-r}, just with the observation that the negative elements of this vector, imply that the matrices to be multiplied are conjugated in the time instant that they represent, which leads to

$$\begin{aligned} &if \quad (a+c)^r \rightarrow \kappa^{+r} = \left[\kappa_1^+, \kappa_2^+, \cdots, \kappa_{k-1}^+, \kappa_k^+\right] \\ &\kappa^+ = \left[\binom{k}{0}, \binom{k}{1}, \binom{k}{2}, \cdots, \binom{k}{k-2}, \binom{k}{k-1}, \binom{k}{k}\right]; \end{aligned} \tag{30}$$

$$\begin{aligned} &if \quad (a-c)^r \rightarrow \kappa^{-r} = \left[\kappa_1^-, \kappa_2^-, \cdots, \kappa_{k-1}^-, \kappa_k^-\right] \\ &\kappa^- = \left[\binom{k}{0}, -\binom{k}{1}, \binom{k}{2}, \cdots, \binom{k}{k-2}, -\binom{k}{k-1}, \binom{k}{k}\right]; \end{aligned} \tag{31}$$

$$\begin{aligned} f_w(\mathbf{\Upsilon}_b^k) = &\left(\mathbf{\Upsilon}_{b,\kappa_1^+}^{k-p}\right)\left(\mathbf{\Upsilon}_{(b-1),1}^{k-p}\mathbf{\Upsilon}_{(b-1),2}^{k-p}\cdots\mathbf{\Upsilon}_{(b-1),\kappa_2^+}^{k-p}\right)\cdots \\ &\left(\mathbf{\Upsilon}_{(b-k-1),1}^{k-p}\mathbf{\Upsilon}_{(b-k-1),2}^{k-p}\cdots\mathbf{\Upsilon}_{(b-k-1),\kappa_{k-1}^+}^{k-p}\right)\left(\mathbf{\Upsilon}_{(b-k),\kappa_k^+}^{k-p}\right), \end{aligned} \tag{32}$$

equation (35), as shown at the bottom of the page. If there is a need to calculate $f_z(\mathbf{\Psi}^k)$ in terms of a matrix $\mathbf{\Psi}^{k-p}$, then $r = p + 1$ is used to calculate the coefficients in κ^{-r}.

Equations (32) and (35) for modulation and demodulation, respectively, are very similar; in the modulation because of the way the DPSK signals are constructed, and in the demodulation because of the use of an auto-covariance detector.

III. CHERNOFF BOUNDARIES

The noise immunity analysis presented below is developed for the MIMO case. The calculation of the exact theoretical curves is really complicated for a higher-order DPSK even for the SISO scenario, and even more for the multiple antenna scenario [12]; this is why a rough approximation of an upper bound for BER is chosen. A rather accurate approximation will be provided, with the possibility of using it for higher-order DPSK and diversity addition application.

The bound proposed is based on the idea of Chernoff boundaries (see, for example, [12]).

The probability of the error for DPSK-1 with an autocovariance detector, for the binary case, can be seen in [9], [12], and it can be approximated (upper bound) as:

$$P_{DPSK1} = \frac{1}{2}\exp\left(-h^2\right), \tag{36}$$

where h^2 is the SNR. Equation (36) shows almost 3db losses, compared with the coherent demodulation.

Using Chernoff Boundaries, the approximation for an upper bound using the autocovariance receiver is

$$P_{Chernoff-DPSK-k} = \exp\left(-\alpha_k h^2\right), \tag{37}$$

where α_k is a parameter calculated for a k order of difference modulation. For DPSK-1, $\alpha_1 = \frac{1}{4}$, so equation (37) becomes

$$P_{Chernoff-DPSK-1} = \exp\left(-h^2/4\right). \tag{38}$$

Similarly, $\alpha_2 = 1/8$ and $\alpha_3 = 1/16$ for DPSK-2 and DPSK-3, respectively.

For the MIMO case, applying a Quadratic Addition for homogeneous diversity branches, one gets [12]:

$$P_e = \frac{L!}{\prod_{i=1}^{L}\left(i + \alpha_k h^2\right)}, \tag{39}$$

where L is the order of diversity; For this work, L will be considered to be equal to the number of receiving antennas, real or virtual. For inhomogeneous cases the solution could also be found at [21].

The parameter α_k and the calculation development of this upper bound, can be seen in Appendix B.

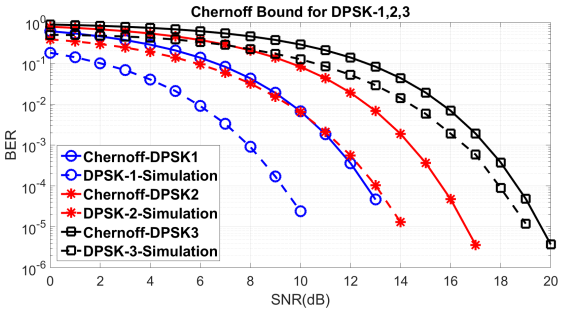

FIGURE 3. Chernoff boundaries for DPSK-1,2 and 3.

IV. SIMULATIONS AND RESULTS

In this section, the simulations and results are presented.

A. EXPERIMENT ONE

It is worth proving the theoretical boundaries proposed in the previous section by means of simulation experiments. That is why a Single Carrier SISO channel scenario is proposed. Based on equation (53), there is a change of value for α_k depending on the order of DPSK desired, and by performing simulations over an additive white Gaussian noise (AWGN) channel; since there is only one antenna, the diversity order $L = 1$ and figure 3 is obtained.

In Fig. 3, it can be seen that for every simulation that represents a different order of DPSK, there is a corresponding curve with an upper bound. The difference between them, at $BER = 10^{-4}$ is not more than $3dB$, which means that it can be considered acceptable, as an upper bound. It can be seen that the curves are getting closer when the differential modulation order is growing; this is not a coincidence, because an approximation in the statistics is made instead of calculating the exact value.

Now, for the MIMO case, the experiments are divided into 2 types: in type A the data matrix is defined as ($\Delta = s\mathbf{I}$), where s is the same symbol along the diagonal, and type B a full matrix is used with different symbols along the diagonal and no zeros on its diagonal. It is worth mentioning, that the type A is not gathering the diversity along the frequency domain, but the type B is gathering it from time, frequency and space domains.

B. EXPERIMENT TWO

In order to see the behavior of DPSK-1 and DPSK-2 against different Doppler frequencies, in Fig. 4 a type-A experiment is considered for a 4×4 MIMO case on a Rayleigh channel with no power delay profile, a constellation size of $M = 8$ and bandwidth of $10MHz$. The difference, for

$$\widehat{\mathbf{\Delta}} = f_{z+1}(\mathbf{\Psi}_b^k) = \left(\mathbf{\Psi}_{b,\kappa_1^-}^{k-p}\right)\overline{\left(\mathbf{\Psi}_{(b-1),1}^{1}\mathbf{\Psi}_{(b-1),2}^{k-p}\cdots\mathbf{\Psi}_{(b-1),\kappa_2^-}^{k-p}\right)}\cdots \overline{\left(\mathbf{\Psi}_{(b-k-1),1}^{k-p}\mathbf{\Psi}_{(b-k-1),2}^{k-p}\cdots\mathbf{\Psi}_{(b-k-1),\kappa_{k-1}^-}^{k-p}\right)}\left(\mathbf{\Psi}_{(b-k),\kappa_k^-}^{k-p}\right). \tag{35}$$

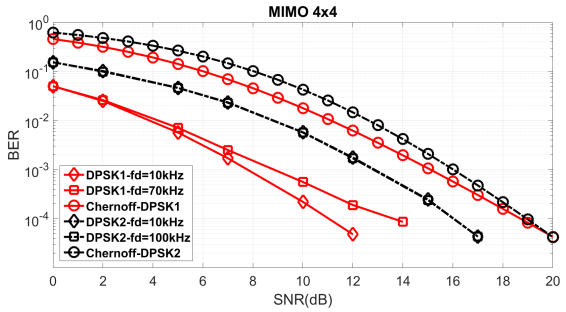

FIGURE 4. Chernoff boundaries and invariance for DPSK-1 and DPSK-2.

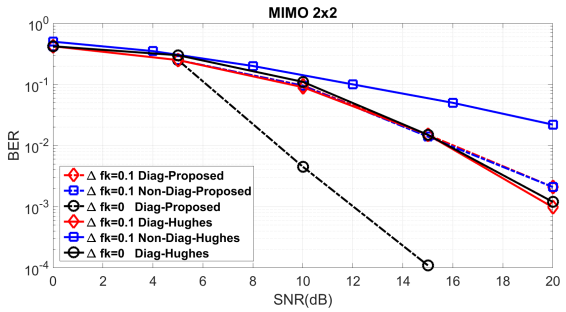

FIGURE 5. Comparison with [10].

DPSK-1, between a Doppler shift of $10kHz$ and $70kHz$, is visible in the performance curves. Remembering that the diversity L, will be equal to the number of receiving antennas. Thus, it can be seen that the system can counteract the Doppler effect, and for DPSK-2 it is actually invariant. It is important to point out that Chernoff bounds are also a good approximation for this case.

C. EXPERIMENT THREE

As can be seen in section II-A, there is a gain in complexity with the proposed method if it is used instead of the one in [10], but in order to evaluate performance, the same conditions are used for both of them, i.e., only using Doppler shifts with AWGN. The experiment is considered for a Single Carrier 2×2 scenario, and two different STBC were taken into consideration: The first one is when only the diagonal of the STBC matrix is used, this can be found in Fig. 5 as "Diag" and will be presented for both methods, the one proposed by Hughes and the one proposed in this work. The other scenario is where the whole STBC matrix is used, written as "Non-Diag" in the same figure, also for both methods. Non frequency shift and frequency shifts are considered for the test. These results are presented in Fig. 5. It can be seen that the proposed method in this work yields the same results if the full STBC matrix is used and not only the diagonal. Meanwhile, with the method in [10] there is a difference if not only the diagonal is used. This means that with a larger MIMO arrangement, not all the possible diversity could be exploited. This difference can be seen in this same simulation when there is an absence of Doppler shift, where there is a clear difference in favor of the work proposed in this paper.

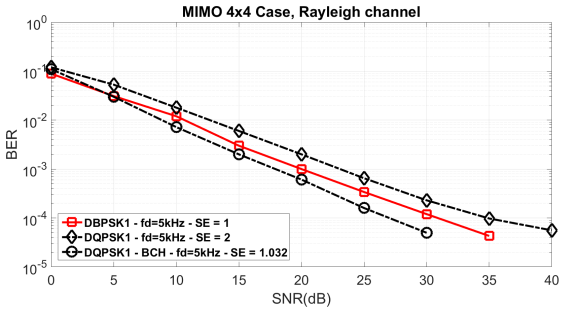

FIGURE 6. Improvement using error correcting codes.

Fig. 5 presents clearly the advantage of using a full matrix to transmit information. It can be seen that the gathering of diversity along the three domains provides really good results and that it is worth continue exploring this path, in contrast to the approach presented in [10].

D. EXPERIMENT FOUR

As mentioned, the autocovariance receiver could bring significant losses due to the increment of noise. Error-correcting codes are a plausible solution to this problem; this work considers BCH(31-16) coding. The considered scenario is a Single Carrier, Type-B experiment, Rayleigh channel, with no delay dispersion, Doppler frequency of 5kHz, bandwidth of $10MHz$, in a 4×4 MIMO array and different values of spectral efficiency.

Thus, in Fig. 6, the square marker represents a realization with no error correcting codes and a constellation of size 2. The diamond and circle markers have the same parameters, both transmitted using a constellation of size 4; just one is being coded and the other is not.

The results show that the gain using error correcting-codes with the same parameters is almost 10dB, while the difference with a smaller constellation is 5dB. Therefore, the use of error-correcting codes represent a good solution to improve BER for DPSK-k, and the low complexity of the proposed receiver confirms that is a correct path to follow. Not leaving aside the fact that the error-correcting codes will have a direct impact in the effect flow of data, since redundancy bits are added and decoded at the receiver.

In Fig. 6, it can be seen that both lines, with markers square and diamond, have almost the same Spectral Efficiency, but there is a 5dB difference between them. This is due to the error-correcting code used. There is always a trade-off, and what we are increasing here is the computational complexity in order to have a better performance in the BER. So, error-correcting codes could be very helpful to improve performance in a non-coherent receiver, if the computational complexity is not an issue.

E. EXPERIMENT FIVE

Finally, transmission over a doubly selective channel is tested. It is worth mentioning that never before has a scalable scheme

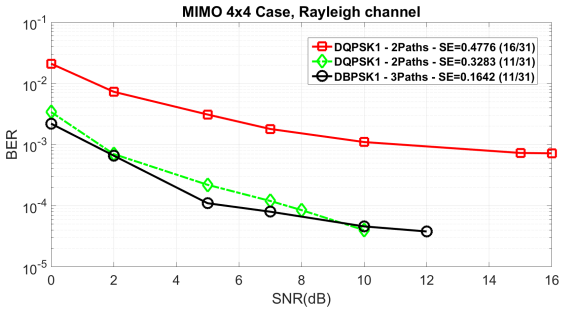

FIGURE 7. Rayleigh channel with multipath delay dispersion and error-correcting codes.

for multiple antennas been presented that uses a simple auto-covariance receiver that could obtain a favorable result over DSC.

Thus, in Fig. 7 a multipath channel is proposed, with the Doppler shift set to $1.5kHz$, an FFT= 64, MIMO 4×4, with paths scattered by $1\mu s$ each, and a virtual trajectory receiver. A type-B experiment is considered, and also BCH codes with a different coding ratio.

It can be seen that while the selectivity increases, the performance falls, which is why the use of error-correcting codes together with the diversity addition of the virtual trajectories proves to be a good option for the system design.

Even though the spectral efficiency is low, the important part to point out is that Fig 7 shows a completely non-coherent 4×4 system over a doubly selective channel, using only an autocovariance receiver and an error correcting code, which has never been presented in the literature.

There is an error floor in Fig. 7. This can be explained by the fact that DPSK requires continuous symbols to demodulate. So, if the first symbol is lost, all the related symbols that depend on it will have an error when the demodulation is done. Since there is selectivity in the three domains, time and frequency, it is impossible to get a better performance by only increasing the SNR, so a technique to reconstruct the lost information should be considered. A better error-correcting code could be a solution, such as Turbo codes.

V. CONCLUSION

This paper has proposed the generalization of a MIMO non-coherent DPSK receiver which takes advantage of diversity over time, frequency and space. This generalization exploits the space-time block codes and at the same time the invariance properties to channel distortions and the capability of using a simple auto-covariance receiver scheme, which results in a communication system of lower complexity, when compared to previous approaches presented in the literature.

The simulation results under doubly selective channels demonstrates the operability of this technique under highly dispersive channels. Furthermore, simulations and Chernoff upper boundaries have shown the invariance properties that DPSK offers; for example, being invariant to Doppler shifts for the second order and showing that for the DPSK-1, it is not completely invariant but it could counteract at some degree this undesired effect. This technique represents an opportunity for the upcoming massive MIMO systems, as it keeps the complexity almost linear with the number of employed antennas.

APPENDIX A
PROOF OF LEMMA

Proof of Lemma 1:

For DPSK-1, the space time modulated matrix is formed by

$$\boldsymbol{\Upsilon}_b^1 = \boldsymbol{\Delta}_b \boldsymbol{\Delta}_{b-1}. \tag{40}$$

For the second order:

$$\boldsymbol{\Upsilon}_b^2 = \boldsymbol{\Upsilon}_b^1 \boldsymbol{\Upsilon}_{b-1}^1 = \boldsymbol{\Delta}_b \boldsymbol{\Delta}_{b-1} \boldsymbol{\Delta}_{b-1} \boldsymbol{\Delta}_{b-2}. \tag{41}$$

Now, using mathematical induction for DPSK-k we have the following equation:

$$\boldsymbol{\Upsilon}_b^k = f_w(\boldsymbol{\Upsilon}^{k-1}) = f_{w-1}(\boldsymbol{\Upsilon}^{k-2}) = \cdots = f_2(\boldsymbol{\Upsilon}^1) = f_1(\boldsymbol{\Delta}), \tag{42}$$

and for DPSK-$(k+1)$:

$$\boldsymbol{\Upsilon}_b^{k+1} = f_{w+1}(\boldsymbol{\Upsilon}^k) = f_w(\boldsymbol{\Upsilon}^{k-1}) = \cdots = f_2(\boldsymbol{\Upsilon}^1) = f_1(\boldsymbol{\Delta}). \tag{43}$$

From equations (42) and (43), it can be seen that for any order of difference modulation, the modulated matrix $\boldsymbol{\Upsilon}_b^k$ can be represented as a function $f_1(\boldsymbol{\Delta}_b)$ of the transmitted symbols.

For the demodulation case, DPSK-1, the following stands:

$$\widehat{\boldsymbol{\Delta}_b} = \mathbf{Y}_b \overline{\mathbf{Y}_{b-1}} = \boldsymbol{\Psi}_b^1 \overline{\boldsymbol{\Psi}_{b-1}^1}. \tag{44}$$

For DPSK-2 we have a similar representation as,

$$\widehat{\boldsymbol{\Delta}_b} = \mathbf{Y}_b \overline{\mathbf{Y}_{b-1}} = \boldsymbol{\Psi}_b^2 \overline{\boldsymbol{\Psi}_{b-1}^2} = \boldsymbol{\Psi}_b^1 \overline{\boldsymbol{\Psi}_{b-1}^1}\, \overline{\boldsymbol{\Psi}_{b-1}^1} \boldsymbol{\Psi}_{b-2}^1. \tag{45}$$

Then, using mathematical induction for receiving data using DPSK-k we have:

$$\widehat{\boldsymbol{\Delta}_b} = f_{z+1}(\mathbf{Y}) = f_z(\boldsymbol{\Psi}^k) = \cdots = f_2(\boldsymbol{\Psi}^2) = f_1(\boldsymbol{\Psi}^1). \tag{46}$$

Receiving data using DPSK-$(k+1)$ can be expressed as

$$\widehat{\boldsymbol{\Delta}_b} = f_{z+2}(\mathbf{Y}) = f_{z+1}(\boldsymbol{\Psi}^{k+1}) = \cdots = f_2(\boldsymbol{\Psi}^2) = f_1(\boldsymbol{\Psi}^1). \tag{47}$$

From (46) and (47), the estimated data can always be represented, in the end, by functions of $f_1(\boldsymbol{\Psi}^1)$.

Then, for the modulated and demodulated signals, a generalization for any order of DPSK can be made using the proposed structure.

Table 3 gives an example of the two first orders of difference modulation and gives an idea of why the matrix construction presented in this work is useful.

TABLE 3. MIMO DPSK-*k* demodulated symbol for STBC.

DPSK-k	$\widehat{\Delta_b}$
$k=1$	$\widehat{\mathbf{\Delta}_b} = \mathbf{\Psi}_b^1 \overline{\mathbf{\Psi}_{b-1}^1} = \mathbf{Y}_b \overline{\mathbf{Y}_{b-1}}$
$k=2$	$\widehat{\mathbf{\Delta}_b} = \mathbf{\Psi}_b^2 \overline{\mathbf{\Psi}_{b-1}^2} = \mathbf{Y}_b \overline{\mathbf{Y}_{b-1}}$ $= \mathbf{\Psi}_b^1 \overline{\mathbf{\Psi}_{b-1}^1}\ \overline{\mathbf{\Psi}_{b-1}^1} \mathbf{\Psi}_{b-2}^1$
$\vdots$	$\vdots$
$k=K-1$	$\widehat{\mathbf{\Delta}_b} = f_z(\mathbf{Y}) = f_{z-1}(\mathbf{\Psi}^{K-1}) = f_{z-2}(\mathbf{\Psi}^{K-2}) = \cdots =$ $= f_3(\mathbf{\Psi}^3) = f_2(\mathbf{\Psi}^2) = f_1(\mathbf{\Psi}^1)$
$k=K$	$\widehat{\mathbf{\Delta}_z} = f_{z+1}(\mathbf{Y}) = f_z(\mathbf{\Psi}^K) = f_{z-1}(\mathbf{\Psi}^{K-1}) = \cdots =$ $= f_3(\mathbf{\Psi}^3) = f_2(\mathbf{\Psi}^2) = f_1(\mathbf{\Psi}^1)$

APPENDIX B
CHERNOFF BOUNDARIES

The principle for this bound is stated by the following expression [12]:

$$\mathbb{E}[X \geq \delta] = \exp(-\nu\delta)\,\mathbb{E}\left[\exp(\nu x)\right] \quad for\ \delta > \mathbb{E}[X], \tag{48}$$

where the parameter ν maximizes equation (48), and it is found by solving the following equation:

$$\mathbb{E}\left[X\exp(\nu x)\right] = \delta\mathbb{E}\left[\exp(\nu x)\right]. \tag{49}$$

Once the parameter ν calculated in equation (49) is found, the following step substitutes for it in equation (48).

The diversity case uses the same calculation for maximizing parameter ν but the bound in equation (48) is stated differently, as in:

$$\mathbb{E}[Y \geq \delta] = \exp(-n\nu\delta)\left[\mathbb{E}\left[\exp(\nu x)\right]\right]^n, \tag{50}$$

where $Y = \frac{1}{n}\sum_{i=1}^{n} X_i$ is a sum of n iid random variables.

For DPSK-1 from [9] the first two statistical moments can be obtained, which is the mean μ and the variance σ^2. In this case $\mu = 0$.

In order to calculate the Chernoff Bound, the value ν must be firstly found; then, using equation (49), it can be found that:

$$\nu = \frac{\delta}{\sigma^2}. \tag{51}$$

Also, in [9], the following equivalences can be found: $\Delta = 2P_s\ h^2 = \Delta/\sigma^2$, $\sigma^2 = N_0/2T$ and $\delta = 2$, where Δ is the variable for the power and h^2 is the SNR.

Thus, equation (48) becomes

$$\mathbb{E}[X \geq \delta] = \exp\left(-\frac{\delta^2}{2\sigma^2}\right). \tag{52}$$

For generalization purposes, equation (52) turns into equation (37), so we have:

$$P_{Chernoff-DPSK-k} = \exp\left(-\alpha_k h^2\right), \tag{53}$$

where α is a variable defined by δ and σ^2, which will change for every order k of DPSK.

If σ^2 from [9] is considered to be the variance of a random variable, the number of times this variance will increase depends completely on the reception method; in this paper the choice was the autocovariance receptor.

Equation (31) can determine the number of times the matrices, for demodulation, have to be multiplied by themselves. Considering this, the number of times the variance will increase for different orders is the sum of the absolute values of the vector in equation (31). According to this, we have

$$\beta_k = 2\sum_{i=1}^{k+1} |\kappa_i^-|, \tag{54}$$

where k is the order of the difference modulation and β is the number of times the variance increases, so it can be expressed by

$$\sigma_k^2 = \beta_k \sigma^2, \tag{55}$$

where σ_k^2 is the value of the variance for a k order difference modulation and $\sigma^2 = \Delta/h^2$ was taken from [9].

A. MIMO CASE

The previous analysis for the SISO case and the calculation of parameter α_k can be taken into consideration, and now for the MIMO case it can be seen from [9] that there is an approximation for the non-coherent case over a Rayleigh channel with L order of diversity. This is expressed as

$$P_e = \frac{1}{2}\frac{L!}{\prod_{i=1}^{L}\left(i + \frac{1}{2}h^2\right)}. \tag{56}$$

Equation (56) is the result of the probability of the error for DPSK-1 with an autocovariance reception stated by equation (36) and the supposition of a Rayleigh channel. If equation (53) and parameter α_k are assumed, equation (56) can be rewritten as equation (39),

$$P_e = \frac{L!}{\prod_{i=1}^{L}\left(i + \alpha_k h^2\right)},$$

giving an approximation for Rayleigh channels with L order of diversity. And for this particular case, the diversity will be considered as the number of receiving antennas in the system, real or virtual.

REFERENCES

[1] J. Wu and P. Fan, "A survey on high mobility wireless communications: Challenges, opportunities and solutions," *IEEE Access*, vol. 4, pp. 450–476, 2016.
[2] F. Pena-Campos, R. Parra-Michel, and V. Kontorovich, "A low complexity multi-carrier system over doubly selective channels using virtual-trajectories receiver," *IEEE Trans. Wireless Commun.*, vol. 15, no. 8, pp. 5206–5217, Aug. 2016.
[3] F. Pena-Campos, R. Parra-Michel, and V. Kontorovitch, "Incoherent DPSK diversity reception in doubly selective channels based on virtual trajectories," *IEEE Trans. Veh. Technol.*, vol. 67, no. 8, pp. 7744–7748, Aug. 2018.
[4] F. Pena-Campos, R. Parra-Michel, and V. Kontorovich, "MIMO multicarrier transmission over doubly selective channels with virtual trajectories receiver," *IEEE Trans. Veh. Technol.*, vol. 68, no. 10, pp. 9330–9338, Oct. 2019.

[5] Y. Mostofi and D. C. Cox, "ICI mitigation for pilot-aided OFDM mobile systems," *IEEE Trans. Wireless Commun.*, vol. 4, no. 2, pp. 765–774, Mar. 2005.
[6] F. Pena-Campos, R. Carrasco-Alvarez, O. Longoria-Gandara, and R. Parra-Michel, "Estimation of fast time-varying channels in OFDM systems using two-dimensional prolate," *IEEE Trans. Wireless Commun.*, vol. 12, no. 2, pp. 898–907, Feb. 2013.
[7] T. Hrycak, S. Das, G. Matz, and H. G. Feichtinger, "Practical estimation of rapidly varying channels for OFDM systems," *IEEE Trans. Commun.*, vol. 59, no. 11, pp. 3040–3048, Nov. 2011.
[8] A. P. Kannu and P. Schniter, "Design and analysis of MMSE pilot-aided cyclic-prefixed block transmissions for doubly selective channels," *IEEE Trans. Signal Process.*, vol. 56, no. 3, pp. 1148–1160, Mar. 2008.
[9] Y. Okunev, *Phase and Phase-Difference Modulation in Digital Communications*. Norwood, MA, USA: Artech House, 1997.
[10] Z. Liu, G. B. Giannakis, and B. L. Hughes, "Double differential space-time block coding for time-selective fading channels," *IEEE Trans. Commun.*, vol. 49, no. 9, pp. 1529–1539, Sep. 2001.
[11] B. L. Hughes, "Differential space-time modulation," *IEEE Trans. Inf. Theory*, vol. 46, no. 7, pp. 2567–2578, Nov. 2000.
[12] J. G. Proakis and M. Salehi, *Digital Communications*. New York, NY, USA: McGraw-Hill, 2008.
[13] J. D. Brown, J. Abouei, K. N. Plataniotis, and S. Pasupathy, "Adaptive demodulation in differentially coherent phase systems: Design and performance analysis," *IEEE Trans. Commun.*, vol. 59, no. 7, pp. 1772–1778, Jul. 2011.
[14] C.-H. Huang and C.-D. Chung, "Diversity transmission and reception of DAPSK for OFDM," *IEEE Trans. Veh. Technol.*, vol. 64, no. 6, pp. 2684–2692, Jun. 2015.
[15] A. M. Rabiei and N. C. Beaulieu, "Frequency offset invariant multiple symbol differential detection of MPSK," *IEEE Trans. Commun.*, vol. 59, no. 3, pp. 652–657, Mar. 2011.
[16] B. Yu, L. Yang, and C.-C. Chong, "Optimized differential GFSK demodulator," *IEEE Trans. Commun.*, vol. 59, no. 6, pp. 1497–1501, Jun. 2011.
[17] C. Xu, D. Liang, S. X. Ng, and L. Hanzo, "Reduced-complexity noncoherent soft-decision-aided DAPSK dispensing with channel estimation," *IEEE Trans. Veh. Technol.*, vol. 62, no. 6, pp. 2633–2643, Jul. 2013.
[18] B. Dimitrijevic, Z. Nikolic, and N. Milosevic, "Performance improvement of MDPSK signal reception in the presence of carrier frequency offset," *IEEE Trans. Veh. Technol.*, vol. 61, no. 1, pp. 381–385, Jan. 2012.
[19] L. Wang and L. Hanzo, "Low-complexity near-optimum multiple-symbol differential detection of DAPSK based on iterative amplitude/phase processing," *IEEE Trans. Veh. Technol.*, vol. 61, no. 2, pp. 894–900, Feb. 2012.
[20] S. Poorkasmaei and H. Jafarkhani, "Orthogonal differential modulation for MIMO multiple access channels with two users," *IEEE Trans. Commun.*, vol. 61, no. 6, pp. 2374–2384, Jun. 2013.
[21] M. K. Simon and M.-S. Alouini, *Digital Communication Over Fading Channels*, vol. 95. Hoboken, NJ, USA: Wiley, 2005.
[22] S. Primak and V. Kontorovich, *Wireless Multi-Antenna Channels: Modeling and Simulation*. Hoboken, NJ, USA: Wiley, 2012.

G. RAMIREZ-ARREDONDO was born in Puruándiro, Michoacán, Mexico, in 1990. He received the B.Sc. degree in electronics from the Universidad Michoacana de San Nicolas de Hidalgo, in 2013, and the M.Sc. degree in electrical engineering specializing in communications and the Ph.D. degree specializing in communications from the Centro de Investigación y de Estudios Avanzados (CINVESTAV), Instituto Politécnico Nacional (IPN), Guadalajara, in 2015 and 2021, respectively. His research interests include digital signal processing, modeling, high mobility MIMO channels, and space-time signal modulation techniques.

F. PEÑA-CAMPOS was born in Guadalajara, Mexico, in 1986. He received the B.Sc. degree in electronics and communications from the University of Guadalajara, in 2008, and the M.Sc. degree in electrical engineering specializing in communications and the Ph.D. degree specializing in communications from CINVESTAV-IPN, Guadalajara, in 2011 and 2015, respectively. His research interests include digital signal processing, modeling, characterization, estimation and equalization of doubly high-mobility MIMO channels, waveform design, and space-time signal modulation techniques.

RAMON PARRA-MICHEL was born in Guadalajara, Mexico, in 1973. He received the B.Sc. degree in electronics and communications from the University of Guadalajara, in 1996, the M.Sc. degree in electrical engineering specializing in communications from CINVESTAV-IPN, Guadalajara, in 1998, and the Ph.D. degree in electrical engineering specialized in digital signal processing for communications from CINVESTAV-IPN, Mexico City, in 2003. He has collaborated with several companies and institutions either in academic or technology projects, such as Siemens, Lucent, Mabe, Mixbaal, Hewlett-Packard, and Intel. He is currently the Director of Guadalajara Unit, CINVESTAV-IPN, and the Head of the Wireless Communication Group. His research interests include modeling, simulation, estimation and equalization of communication channels, and digital implementation of DSP algorithms for communication systems.

VALERI KONTOROVICH (Life Fellow, IEEE) was born in Sverdlovsk, Russia. He received the M.S.E.E., Ph.D., and Dc.Sc. degrees from the St. Petersburg State University of Telecommunications (St. Pt. UT). From 1964 to 1965, he was a Technical Staff Member of the State Radio Institute. In 1965, he joined St. Pt. UT, where he founded the Laboratory of Electromagnetic Compatibility (EMC lab), in 1976. In 1984, the laboratory was transformed into Branch Lab of the Ministry of Telecommunications of the former USSR. From 1992 to 1995, he was the Head of Department of Radio Receivers and EMC, where he has been a Full Professor, since 1988. Since 1993, he has been a Full Professor at CINVESTAV-IPN, Mexico. He is currently an Emeritus National Researcher. He has published eight books and more than 300 journal articles and conference papers. He holds 26 patents. His current research interests include electromagnetic compatibility of radio communication systems, interference analysis, channel modeling, statistical theory of communications, and cognitive radio networks. He is a member of the Mexican Academy of Sciences.